

Removing EOG Artifacts from EEG Signals Using a Modified Wavelet-RLS Method

Maryam Tavakoli¹, Hamed Ahani²

¹Department of Mechanical Engineering and Engineering Science, Yazd University, Yazd, Iran
Yazd Province, Yazd, Safaeih, Iran

²Department of Mechanical Engineering and Engineering Science, University of North Carolina at Charlotte, Charlotte, NC, USA

Correspondence to: Ahani H. (E-mail: hahani@uncc.edu)

Abstract

EEG signals are among the weakest and most disturbing vital signals because with the slightest change in body posture, and various artifacts will be added to them. The presence of artifacts in the EEG signal leads to an incorrect analysis of this signal. Due to the importance of the subject, various methods have been proposed to eliminate these artifacts. In this thesis, the Wavelet-RLS modified method for removing eyelid articulation from the EEG signal is improved. We then compare the performance of the modified Wavelet-RLS method with the SNR and MSE criteria with the RLS and regular Wavelet-RLS methods. In this method, first, the noise signal is analyzed by the wavelet. Then the coefficients in the frequency bands, including the blinking effect, are filtered by a recursive least squares (RLS). Finally, the clean signal is reconstructed with the inverse Wavelet transformation. The results show that the performance of the modified Wavelet-RLS method is better than the regular Wavelet-RLS and RLS methods in terms of MSE and SNR.

Keywords: Noise filtering, Electroencephalogram, Adaptive filter

Received: 26 May 2020, Accepted: 19 June 2020

DOI: 10.22034/jbr.2020.232798.1022

1. Introduction

The recording of electrical activity of the brain is called Electroencephalogram (EEG), which is associated with artifacts such as articulation of the eyelids, artifacts caused by the electrical activity of muscles, artifacts caused by the electrical activity of the heart, and so on. According to the fact that the eyelid artifact has a larger amplitude than the EEG signal, it can affect the quality of the signal recorded from all electrodes, even the back of the head [1].

The blinking effect occurs with a range of more than 800 microvolts and a time interval of 20-40 milliseconds [2]. In 1996, Makeig and colleagues proposed an independent component analysis (ICA) method to eliminate artifacts from electrical muscle activity and eyelid artifact. They visually identified the sources of artifact effect after finding the independent sources by decomposing ICA analysis. They reconstructed the pure signal by combining the remaining components and resetting the columns of combining matrix to the zero corresponding to the



This work is licensed under a [Creative Commons Attribution-NonCommercial-NoDerivatives 4.0 International License](https://creativecommons.org/licenses/by-nc-nd/4.0/).

rows of noise sources [3]. It must be considered that in the communication link, the size of the transferred data is important. Therefore, in the measurement hardware, the compression methods are used for creating fast data transmission. According to the [4], to increase the data transmission rate and simplicity of the compressors, the nominal system architecture can generate compressed ECG samples in a linear method and with CR 75%. The blinking effect can be propagated in the acquired signal without considering an appropriate compression method [4]. The proposed approach in [4] is an effective solution for the communication link.

In 2002, Zikove and colleagues provided a way to remove EOG from the EEG signal using wavelet conversion. First of all, they analyzed the noise signal by converting the Stationary Disconnected Wavelet (SWT). Then, they performed the thresholding operation on the coefficients in the low-frequency bands and finally reconstructed the clean signal [5]. Mohamed et. al. [6, 7] studied frequency response of sensors connected to a structure in a broad range of frequencies and eliminated noise signals before implementing Fast Fourier Transformation. In [8], the application of the time-frequency transforms presented for efficient recovery of structural health monitoring on Kronecker Compressive sensing. Also, these transformations are used for system identification and FDIR studies [9,10].

In 2004, a method based on adaptive filters to remove the EOG effect from the brain signal was developed. A Class 3 RLS filter was used, and the results of the experiments indicated that the proposed method, in addition to stability, has rapid convergence and simplicity in implementation [11]. Nowadays, a combination of EEG signals is used to improve the EOG artifact removal process. Marku g Nazerth used a combination of ICA and Violet methods in 2006 to remove the artifact from the EEG signal. They first applied ICA to the noise signal and then removed the noise components detected by eye observation using wavelet thresholds [12]. The problem of this method is that it is not applicable in a single-channel recorder. Babu and Parasad proposed the wavelet-RLS hybrid method in 2011 to remove the EOG artifact from the EEG signal. They decomposed the noise EEG signal

from the EOG signal by wavelet, which was recorded simultaneously with the noise signal. Then the RLS filter was applied to all samples obtained from the wavelet decomposition. Finally, they captured the pure signal from the difference between the estimated noise signal and the estimated EOG and compared the proposed method with the RLS method. The results showed that the proposed method performs better than the RLS method in terms of MSE [13]. In 2016, Adnani and colleagues used Butterworth low pass digital to remove noise from the signal and obtain a pure signal for further processing. Then, signal decomposed into another section called Instinct Mode Function (IMF) and were tested by using the Instantaneous Frequency (IF) [14]. These methods can be used in other applications, for instance, in biomedicine [15].

In the present study, in order to improve the elimination of artifact, the Wavelet-RLS method is applied in order to simulate the results in terms of MSE and SNR. For this purpose, after analyzing the wavelet results, the RLS filter is applied only to the coefficients in the low-frequency bands. An optimal RLS filter is used for each frequency band in terms of the order. The clean signal is then reconstructed by inverse wavelet conversion. Section 2 describes the methods and simulation methodology, and the results are presented and discussed in sections 3 and 4, respectively.

2. Methodology

2.1. Adaptive Filter

The block diagram of the adaptive filter is shown in Figure (1) [11, 16]. In this primary input method, $S(n)$ is a linear combination of the clean and noisy signal. Two reference inputs, VEOG and HEOG are compatible. Two filters with limited impulse response have length M (two filters can have lengths). The output of the filter is adaptive as obtained in the following equation:

$$e(n) = s(n) - \hat{r}_v(n) - \hat{r}_h(n) \quad (1)$$

Where the filtered reference signals are expressed as follows:

$$\hat{r}_v(n) = \sum_{m=1}^M h_v(m)r_v(n+1-m) \quad (2)$$

$$\hat{r}_h(n) = \sum_{m=1}^M h_h(m)r_h(n+1-m) \quad (3)$$

Assuming that x is a random signal with the mean value of zero and unrelated to r_v , r_h , and the noise of z , the mathematical relation can be written as follows:

$$E(e^2) = E[(X + Z - \hat{r}_v - \hat{r}_h)^2] = E(X^2) + E[(Z - \hat{r}_v - \hat{r}_h)^2] \quad (4)$$

In the RLS algorithm, instead of minimizing the above functions, the objective function should be minimized:

$$\epsilon(n) = \sum_{i=M}^n \lambda^{n-i} e^2(i) = e^2(n) + \lambda e^2(n-1) + \dots + \lambda^{n-M} e^2(M) \quad (5)$$

Where lambda is the forgetting factor, M is the order of filter, and n is the number of signal samples. The forgetting factor is obtained from the following equation.

$$\lambda^n = 0.5 \quad (6)$$

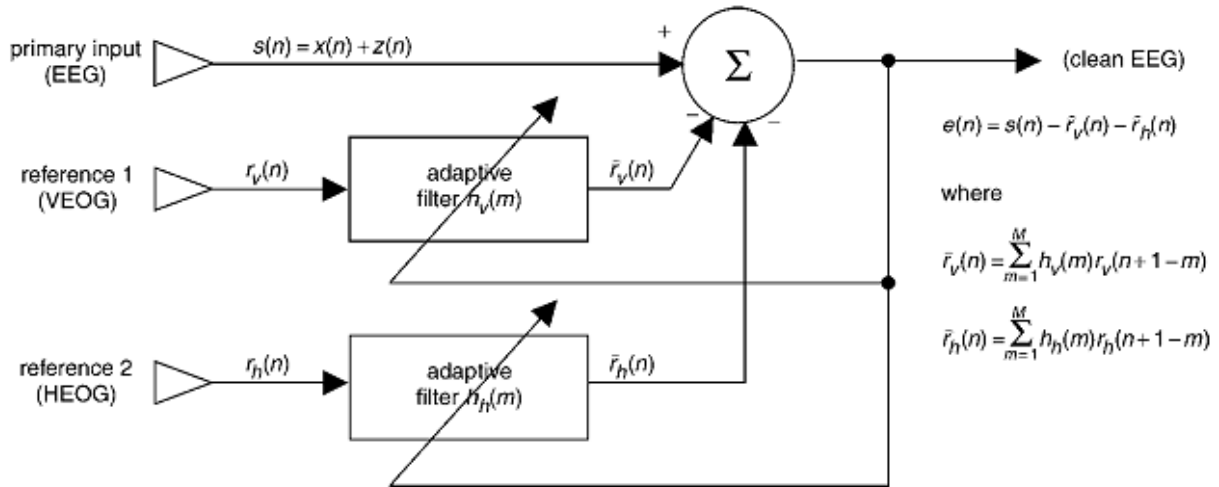


Figure 1. Schematic block diagram of the adaptive noise filter with two reference inputs

Table 1. The mean values of MSE and SNR in 4 different channels by RLS method

Criterion	F _z	F _{c_z}	C _z	P _z
MSE	6.5 ±2.2	5.1 ±1.3	4.3 ±1.5	3.8 ±1.4
SNR	3.7 ±2.2	5.7 ±1.7	7.5 ±2	7.6 ±2.7

2.2. Wavelet-RLS Method

The wavelet conversion is one of the most powerful tools used in noise elimination [17, 18]. In the reference article [13], the expression of RLS in the field of wavelet has better results than RLS. The procedure in the Wavelet-RLS combination method is as follows:

- 1- To apply SWT on noisy signal and reference EOG
- 2- To implement RLS filter on all coefficients obtained from wavelet conversion and the noise of EOG estimation
- 3- Inverse wavelet conversion of the signal in step 2
- 4- To extract clean signal by subtracting of step 3 from step 1

2.3. Optimized Wavelet-RLS Method

According to the fact that the effect of the EOG artifact is in frequency bands below 20. A RLS filter was applied for the coefficients in these frequency bands in order to improve the process of mitigating the artifact (an optimal RLS filter is designed for each band

regarding the order). The steps to eliminate EOG artifact by a compound method is as follow:

- 1- To apply SWT on noisy signal and reference EOG
- 2- To implement RLS filter on all coefficients in frequency bands of artifact
- 3- To substitute the existing coefficient in artifact frequency bands in step 1 with corrected coefficients in step 2
- 4- Recovery of the clean signal by inverse wavelet conversion

2.4. Data and Signal Simulation

The data used in this study is from the data collection of Ila BCI2008 competition [19]. This data includes nine people and 22 EEG channels and 3 EOG channels for each person, which the second EOG channel represents the artifact.

These signals are sampled at 250 Hz and filtered by a transient filter with a frequency range of 0.5-100 Hz. A 50 Hz band-stop filter was used to remove the mains electricity noise. Figure 2 shows how to apply electrode and record EEG signals with a 10-20 standard [19].

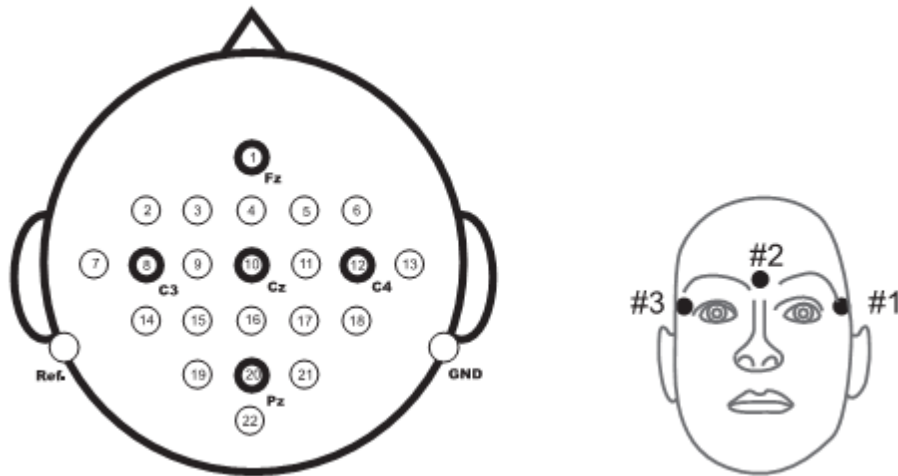


Figure 2. The method of instalment of Electrode

To compare the methods, we need the initial clean signal and simulated signals. In this study, we separated visually 2,000 sample signals for 5 individuals and 4 channels (channels Fz-FCz-Cz-Pz).

Besides, for each person, 2000 samples are separated from the EOG channel. To eliminate artifacts above 450 Hz, we passed the EEG signals through a low-pass filter of 45 Hz. Another low-pass filter of 20 Hz was used to filter the EOG signal [20].

EOG as a weight function was added to the clean signal to simulate the noise signal. EOG weight for each channel of ICA decomposition is obtained. The number of independent sources with the linear composition are obtained by observing of the signal. ICA relationships are formulated as follows:

$$S = A * X \quad (7)$$

$$X = W * X \quad (8)$$

In the above relations X is the vector of observations and the only known of the problem, A as the separating matrix, S represents the independent sources, and W is the compound matrix. After initial diagnosis of noise, the column of W , which corresponds to the noise source line, eliminated from the same EOG coefficients for each channel. Given that the coefficients obtained are applied to the registered EOG channel, not the assumed EOG source in the ICA, therefore, all the coefficients are related. Due to the EOG effect in different channels, they are normalized to the coefficients of the EOG channel.

3. Results

In this section, to compare the methods of two criteria, we used the mean squares error (MSE) and the signal-to-noise ratio (SNR) as shown below. [21, 22].

$$MSE = \frac{\sum_{n=1}^N [e(n) - x(n)]^2}{N} \quad (9)$$

$$SNR = 20 * \log_{10} * \left(\frac{\sqrt{\text{mean}(e(n))^2}}{\sqrt{\text{mean}(e(n) - x(n))^2}} \right) \quad (10)$$

In the above relations, the $e(n)$ signal of noise removal, N the number of signal's samples and $x(n)$ is the initial

clean signal. Regarding the above relationships, smaller MSE and larger SNR, lead to better output.

3.1. The Results of RLS Method

In the RLS algorithm, two parameters, M and Lambda, are considered. Due to Equation 6, the lambda value was obtained 0.99. The order of the filter is calculated experimentally. In this study, after evaluating orders 3, 6 and 12 and as RLS filter order, the order 3 was selected as the optimum order.

A sample of noisy signal and cleaned signal by RLS for the second individual in channel number 4 was shown in figure 3.

The MSE and SNR values for the RLS method are shown in Table 1.

3.2. The Result of Wavelet-RLS

In order to remove the artifact by the Wavelet-RLS method, as in the reference article [13], the following procedure was performed.

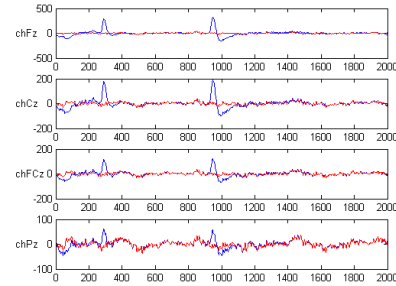


Figure 3. Noise filtering by RLS, Noisy signal (Blue line), filtered signal (red line)

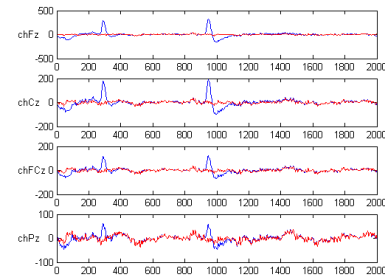


Figure 4. Noise filtering by Wavelet-RLS, Noisy signal (Blue line), filtered signal (red line)

- 1- Noisy signal and reference EOG, recorded simultaneously, were decomposed to order 4 by SWT and mother wavelet of system3
- 2- To implement RLS filter on all coefficients obtained from wavelet conversion and the noise of EOG estimation
- 3- Inverse wavelet conversion of the signal in step 2
- 4- To extract clean signal by subtracting of step 3 from step 1

Figure 4 shows the noisy signal and cleaned signal by wavelet-RLS for second individual in channel number 4.

The table 2 represent the values of the MSE and SNR for the Wavelet-RLS method.

3.3. The Results of the Optimized Wavelet-RLS Method

The procedure to optimize the Wavelet-RLS is as follow:

- 1- Noisy signal and reference EOG, recorded simultaneously, were

decomposed to order 4 by SWT and mother wavelet of system3.

- 2- The existing coefficients in 4th order, which are in the frequency range [0-15.6] and [15.6-30.2] Hz, are filtered by RLS. The coefficients obtained from step one was used as reference inputs for filters. The 3rd order filter for frequency range [0-15.6] and 1st order for [15.6-30.2] are applied. The orders were selected after evaluation of order 1, 3 and 6.
- 3- The obtained coefficients from step 2 were substituted by 4th order coefficients from step 1.
- 4- To recover the clean signal by inverse wavelet conversion.

Figure 5 depicts the noisy signal and cleaned signal by the proposed method for the second individual in channel number 4.

The values of the MSE and SNR for the optimized Wavelet-RLS method are shown in table 3.

Figures 6 and 7, respectively, illustrate the comparison between the average of SNR and MSE for 5 persons in different channels in three different methods.

Table 2. The mean values of MSE and SNR in 4 different channels by Wavelet-RLS method

Criterion	Fz	Fcz	Cz	Pz
MSE	5.1 ±1.6	4.7 ±1.4	4.1 ±1.5	3.6 ±1.3
SNR	6.3 ±1.3	6.8 ±1.1	8 ±1.6	8.3 ±2.3

Table 3. The mean values of MSE and SNR in 4 different channels by optimized Wavelet-RLS method

Criterion	Fz	Fcz	Cz	Pz
MSE	4.6 ±4.4	4.5 ±1.4	3.7 ±1.7	3.1 ±1.6
SNR	7.3 ±1.7	8.0 ±1.8	8.9 ±2.2	9.7 ±2.9

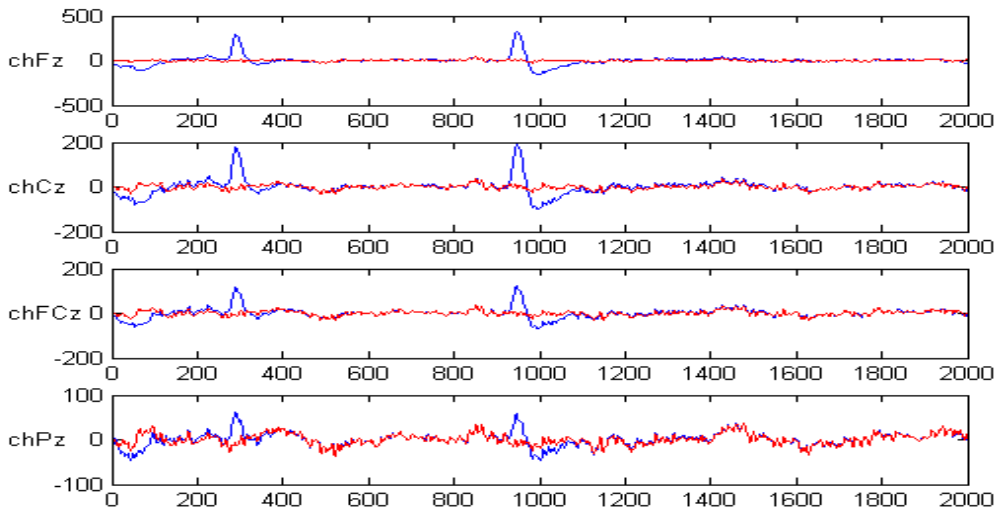


Figure 5. Noise filtering by optimized Wavelet-RLS, Noisy signal (Blue line), filtered signal (red line)

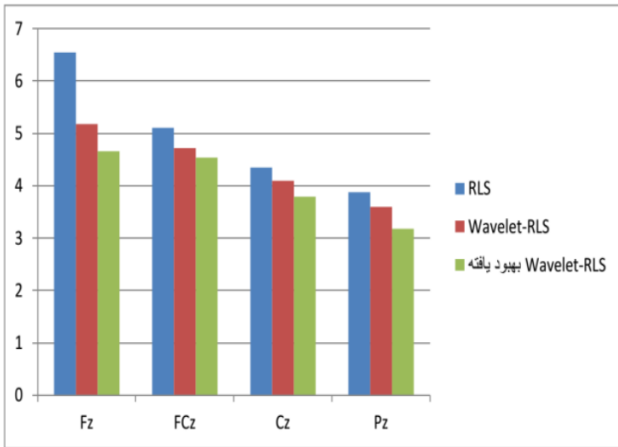


Figure 6. The mean values of MSE for three artifact filtering methods

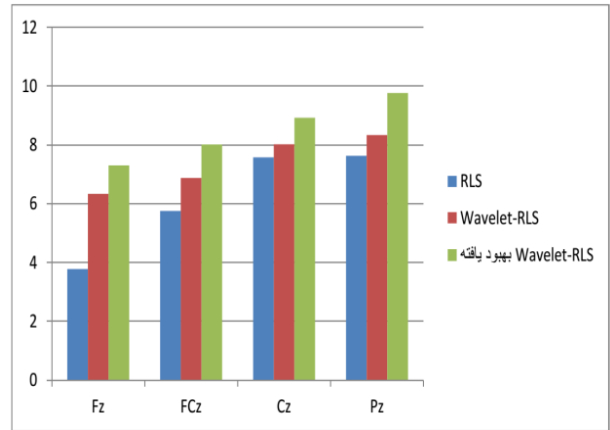


Figure 7. The mean values of SNR for three artifact filtering methods

4. Conclusion

In this paper, the Wavelet-RLS method was optimized in order to eliminate artifacts EOG from EEG signal. The proposed method in this study has the advantage of having multiple RLS filters for each frequency band compared to the method proposed in [13]. Moreover, unlike reference [13], in the present article, the clean signal is obtained by RLS from the difference between the noise signal and the estimated EOG inverse wavelet conversion and high-frequency bands. The values of MSE and SNR are obtained by applying the method on a series of simulated data To evaluate this method. The results show that optimized Wavelet-RLS has better performance as the matter of MSE and SNR compared to the RLS and Wavelet-RLS methods.

Conflict of interest

The authors certify that they have no affiliations with or involvement in any organization or entity with any financial interest, or non-financial interest in the subject matter or materials discussed in this manuscript.

Acknowledgments

No applicable.

References

- [1] Wallstrom GL, Kass RE, Miller A, Cohn JF, Fox NA. Automatic correction of ocular artifacts in the EEG: a comparison of regression-based and component-based methods. *International journal of psychophysiology*. 2004 Jul 1;53(2):105-19.
- [2] Knight JN. Signal fraction analysis and artifact removal in EEG (Doctoral dissertation, Colorado State University).
- [3] Makeig S, Bell AJ, Jung TP, Sejnowski TJ. Independent component analysis of electroencephalographic data. In *Advances in neural information processing systems* 1996 (pp. 145-151).
- [4] Izadi V, Shahri PK, Ahani H. A compressed-sensing-based compressor for ECG. *Biomedical engineering letters*. 2020 Feb 6:1-9.
- [5] Zikov T, Bibian S, Dumont GA, Huzmezan M, Ries CR. A wavelet based de-noising technique for ocular artifact correction of the electroencephalogram. In *Proceedings of the Second Joint 24th Annual Conference and the Annual Fall Meeting of the Biomedical Engineering Society* [Engineering in Medicine and Biology 2002 Oct 23 (Vol. 1, pp. 98-105)]. IEEE.
- [6] MOHAMED AF, MODIR A, SHAH KY, TANSEL I. Control of the Building Parameters of Additively Manufactured Polymer Parts for More Effective Implementation of Structural Health Monitoring (SHM) Methods. *Structural Health Monitoring* 2019. 2019..
- [7] Mohamed AF, Modir A, Tansel IN, Uragun B. Detection of Compressive Forces Applied to Tubes and Estimation of Their Locations with the Surface Response to Excitation (SuRE) Method. In *2019 9th International Conference on Recent Advances in Space Technologies (RAST) 2019 Jun 11 (pp. 83-88)*. IEEE.
- [8] Surakanti SR, Khoshnevis SA, Ahani H, Izadi V. Efficient Recovery of Structural Health Monitoring Signal based on Kronecker Compressive Sensing. *International Journal of Applied Engineering Research*. 2019;14(23):4256-61.
- [9] Izadi V, Abedi M, Bolandi H. Verification of reaction wheel functional model in HIL test-bed. In *2016 4th International Conference on Control, Instrumentation, and Automation (ICCIA) 2016 Jan 27 (pp. 155-160)*. IEEE.
- [10] Izadi V, Abedi M, Bolandi H. Supervisory algorithm based on reaction wheel modelling and spectrum analysis for detection and classification of electromechanical faults. *IET*

- Science, Measurement & Technology. 2017 Aug 1;11(8):1085-93.
- [11] He P, Wilson G, Russell C. Removal of ocular artifacts from electro-encephalogram by adaptive filtering. *Medical and biological engineering and computing*. 2004 May 1;42(3):407-12.
- [12] Castellanos NP, Makarov VA. Recovering EEG brain signals: artifact suppression with wavelet enhanced independent component analysis. *Journal of neuroscience methods*. 2006 Dec 15;158(2):300-12.
- [13] Babu PA, Prasad KV. Removal of ocular artifacts from EEG signals by fast RLS algorithm using wavelet transform. *International Journal of Computer Applications*. 2011 May 4;21(4):1-5.
- [14] Adnani AA, Dokami A, Morovati M. Fault detection in high speed helical gears considering signal processing method in real simulation. *Latin American Journal of Solids and Structures*. 2016 Nov;13(11):2113-40.
- [15] E. Ahani, T. Toliyat, M. Mahmoudi Rad, “Comparing size particle, release study and cytotoxicity activity of PHMB encapsulated in different liposomal formulations: neutral and cationic liposomes”, *Bioengineering Research*, 1(3) (2019) 1-6.
- [16] Ahani H, Familian M, Ashtari R. Optimum Design of a Dynamic Positioning Controller for an Offshore Vessel. *Journal of Soft Computing and Decision Support Systems*. 2020 Feb 6;7(1):13-8.
- [17] Sheikhshahrokhdehkordi M, Goudarzi N, Saffaraval F, Mousavi sani S, Tkacik P. A TomoPIV Flow Field Study of NACA 63-215 Hydrofoil With CFD Comparison. *InFluids Engineering Division Summer Meeting 2019 Jul 28 (Vol. 59070, p. V004T04A039)*. American Society of Mechanical Engineers.
- [18] Mousavi sani S, Goudarzi N, Sheikhshahrokhdehkordi M, Bisel T, Dahlberg J, Tkacik P. Exploring and Improving the Flow Characteristics of an Empty Water Channel Test Section: The Application of TomoPIV and Flowrate Sensors for Whole-Flow-Field Visualization. *InFluids Engineering Division Summer Meeting 2019 Jul 28 (Vol. 59070, p. V004T04A040)*. American Society of Mechanical Engineers.
- [19] Brunner C, Leeb R, Müller-Putz G, Schlögl A, Pfurtscheller G. BCI Competition 2008–Graz data set A. Institute for Knowledge Discovery (Laboratory of Brain-Computer Interfaces), Graz University of Technology. 2008;16.
- [20] Shahabi H, Moghimi S, Zamiri-Jafarian H. EEG eye blink artifact removal by EOG modeling and Kalman filter. *In2012 5th International Conference on BioMedical Engineering and Informatics 2012 Oct 16 (pp. 496-500)*. IEEE.
- [21] He P, Kahle M, Wilson G, Russell C. Removal of ocular artifacts from EEG: a comparison of adaptive filtering method and regression method using simulated data. *In2005 IEEE Engineering in Medicine and Biology 27th Annual Conference 2006 Jan 17 (pp. 1110-1113)*. IEEE.
- [22] Jiang X, Bian GB, Tian Z. Removal of artifacts from EEG signals: a review. *Sensors*. 2019 Jan;19(5):987.